J. Marine Sci. Appl. (2012) 11: 24-33
DOI: 10.1007/s11804-012-1102-9

The Effects of Flexible Vegetation on Forces with a Keulegan-Carpenter Number in Relation to Structures Due to Long Waves

Noarayanan Lakshmanan[1], Murali Kantharaj[2] and Vallam Sundar[2*]

1. Division of Environmental & Water Resources Engineering, Nanyang Technological University, Singapore 63979, Singapore
2. Department of Ocean Engineering, Indian Institute of Technology Madras, Chennai 600036, India

Abstract: Extreme coastal events require careful prediction of wave forces. Recent tsunamis have resulted in extensive damage of coastal structures. Such scenarios are the result of the action of long waves on structures. In this paper, the efficiency of vegetation as a buffer system in attenuating the incident ocean waves was studied through a well controlled experimental program. The study focused on the measurement of forces resulting from cnoidal waves on a model building mounted over a slope in the presence and absence of vegetation. The vegetative parameters, along with the width of the green belt, its position from the reference line, the diameter of the individual stems as well as the spacing between them, and their rigidity are varied so as to obtain a holistic view of the wave-vegetation interaction problem. The effect of vegetation on variations of dimensional forces with a Keulegan-Carpenter number (*KC*) was discussed in this paper. It has been shown that when vegetal patches are present in front of structure, the forces could be limited to within $F^* \leq 1$, by a percentile of 92%, 90%, 55%, and 96%, respectively for gap ratios of 0.0, 0.5, 1.0, and 1.5. The force is at its maximum for the gap ratio of 1.0 and beyond which the forces start to diminish.
Keywords: Coastal vegetation; modeling vegetal stems; vegetation–flow parameter; vegetal parameter; staggered vegetation; Keulegan-Carpenter number
Article ID: 1671-9433(2012)01-0024-10

1 Introduction

The vegetation on the seaside of existing structures during the ingress of the great Indian Ocean tsunami acted as buffers in reducing the inundation heights and distance into the land. This phenomenon is not well understood. Furthermore, as a part of the mitigation measurements, the information of run-up distance and heights affected by vegetation is needed. This need has prompted the authors to carry out an experimental investigation.

(Hiraishi and Harada, 2003) carried out tests in a tsunami channel to investigate the efficiency of a chemical porous medium representing a greenbelt barrier in reducing the run-up and inundation distance. It was claimed that the greenbelt had a similar efficiency in reducing the incident energy as that of coastal dikes composed of wave energy dissipating blocks.

Additionally, using the 1998 Papua New Guinea tsunami data, a numerical simulation with a nonlinear long wave model that included the drag force terms was carried out to study the application of a greenbelt. The maximum tsunami run-up height on shore was reported to be smaller in the presence of a greenbelt compared to where there was no protection. Through physical model experiments in a flume with model mangrove trees and two-dimensional depth-integrated numerical modeling, Struve *et al*. (2003) showed that the drag coefficient may increase with an increase in the tree surface. After the December 26, 2004 Indian Ocean tsunami, a survey along 18 coastal hamlets along the southeast coast of India carried out by (Kathiresan and Rajendran, 2005) revealed that the presence of mangroves and other plantations had significantly reduced the tsunami height and its inundation into the coastal area. Based on their studies, the plant species that need to be planted along the coast as a mitigation measure were identified. The results of a field survey on the effects of the above tsunami along the coast of Thailand as well as on the aspects of the role of vegetation or a greenbelt were discussed by (Hiraishi, 2005). The study also covered the applicability of a greenbelt as a tsunami mitigation measure was demonstrated through a numerical model, according to which the eroded volume at a beach with some vegetation was found to be smaller than at a beach without vegetation. It was also pointed out that the stabilization of sandy beaches is another positive impact of a greenbelt for tsunami disaster mitigation. An overview on the effectiveness of mangroves and coastal forests in reducing tsunamis along with evidence for its effectiveness against tsunamis was reported by (Kongko, 2005). It was claimed that mangrove and casuarinas plantations attenuated tsunami-induced run-up and height and protected shorelines against damage. The work of Danielsen *et al*. (2005) for the tsunami affected district of Cuddalore, Tamil Nadu, on the southeast coast of India serves as a proof for the mangrove and casuarinas

Received date: 2011-06-17.
***Corresponding author Email:** vsundar@iitm.ac.in

plantations which acted as tsunami attenuators and protected shorelines against damage. (Harada and Imamura, 2005) quantitatively evaluated the hydrodynamic effects and damage-prevention functions of coastal forests against tsunamis with a view of using them as tsunami counter measures and reported that an increase in forest width can reduce not only inundation depth, but also the currents and hydraulic forces behind a coastal forest. (Nandasena and Tanaka, 2007) analyzed two different coastal species, *Pandanus odoratissimus* and *Cocos nucifera*, which are dominant in Sri Lanka, through numerical studies to understand the hydrodynamic behavior of these species in the case of the propagation of a tsunami. Tanaka *et al*. (2007) studied the effects of coastal vegetation on tsunami damage based on field observations carried out after the Indian Ocean tsunami on December 26, 2004 along the southern coast of Sri Lanka. Sundar *et al*. (2007) conducted a signature study along the coast of Tamil-nadu (southeast coast of India) and the Andaman and Nicobar Islands which also covered the effect of vegetation on the inundation distance and heights due to the great Indian Ocean tsunami of 2004. Augustin *et al*. (2009) reported the mean drag coefficients for emergent and nearly emergent wetland vegetation as a function of Reynold's number. Irtern *et al*. (2009), by adopting cylindrical timber members representing coastal forests, investigated their effects in the reduction of run-up due to the ingress of a tsunami. (Tanino and Nepf, 2008) reported the variations in the mean drag coefficients for submerged vegetation exposed to steady flow.

The stiffness of the vegetation is one of the major parameters that govern its interaction with flow, an aspect needing immediate attention and which has been considered in the present physical model study to understand how the vegetal drag influences the flow behavior. In the present work, the rigidity of the vegetation has been modeled in order to have a better understanding of its attenuation characteristics and further allow the application of the results from model study to real world situations. The vegetation issue is neither species nor location specific, but depends only on the characteristics of flow and vegetation.

2 Conceptualization

The predominant physical processes in the problem chosen are the bending action of the vegetation, wake induced vibrations on the downstream of the Korman vortex street, and the proximity effect due to the presence of the neighboring structures in the flow field. To account for these processes, rigidity must be modeled and a suitable (SP/*D*) ratio should be identified. The canopy of a tree that would also contribute some resistance to the flow and the skin friction in real situations is not modeled in the present study. While doing wave flume experiments, the wind effect is totally ignored.

Thus, the present study focuses on the understanding of the interaction of vegetation with Cnoidal waves.

3 Experimental investigations

3.1 Physical variables and dimensionless parameters

Quantification of the friction factor and energy loss past vegetation is of primary interest and has practical relevance as far as long waves are concerned. However, when determining the forces on the structures mounted at a distance from the shoreline/reference line, with the presence and absence of vegetation, a number of wave and beach parameters should be considered. The following variables of vegetal response are of interest for both currents and waves.

$$\text{Force} = f(\rho, g, h, H, T, B_s, D, D_b, \text{BG}, f_1, l, \text{SP}, E, L, \beta, R_u, V) \quad (1)$$

where, the Force represents maximum forces acting on the structure behind the vegetal patch; ρ = mass density of water; g = gravitational acceleration; h = depth of water in the flume; H = wave height; T = wave period; B_s = width of the structure; D = diameter of the vegetation; D_b = diameter at the root of the vegetation; BG = width of green belt; f_1 = frequency of the first mode of the vegetal stem; l = height of the vegetation; SP = center to center spacing between vegetation; E = modulus of plant stiffness; L = wave length; β = beach slope; R_u = run-up; V = flow velocity or $U_{\max}$ being maximum orbital velocity under waves.

Herein, h refers to h_s which is the depth of the water at the toe of the structure. The variables seen in Eq.(1) are grouped according to Buckingham's Pi theorem. The parameters thus obtained are tabulated in Table 1, in which L_o is the deep water wave length. The non-dimensional wave force on structure F^* is as defined below.

$$F^* = \left(\frac{F_{\max}}{0.5 \times \rho g H^2 B_s} \right) \quad (2)$$

Table 1 Non-dimensional parameters and their ranges for the present study

Parameters	Values considered
$KC = [(U_{\max} T)/B_s]$	31–145
Vegetation flow parameter, VFP= $[EI(\text{BG}/D)]/[\rho H l^3 V_{\text{avg}}^2(\text{SP}/D)]$	0.006–2.31
Vegetal parameter = $[(\text{BG}\times\text{SP})/D^2]$	94–8333
Reduced velocity, $V_r = [V_{\text{avg}}/(f_1 D_t)]$	11–166

3.2 Modeling the Green Belt

Motivated by the need to study the hydro-elastic interaction of the flow with vegetal stems, a suitable material for the model had to be identified to represent coastal vegetation in the real world. One of the guiding parameters for this purpose is Young's modulus, E. The common timber would

have an E value in the range from 10.05 GPa to 15 GPa. The mangrove has one of the highest E values at 20.03 GPa. In order to cover this wide range of E, a reference value of 14GPa has been assumed for the field which had to be modeled for laboratory tests. In order to scale down the prototype values and identify the model material, assuming that the flow is due to a storm surge or tsunami, and considering also the experimental ranges of flow (including velocities and flow depth), a guiding scale ratio of 1:40, was adopted. This would mean that the E value for the model material should be about 0.35 GPa, which is quite difficult to identify.

The most practical option for achieving the above scale is to consider EI as a single parameter and by scaling the rigidity. For the present study the material considered is Poly Ethylene with an E value of about 3.8 GPa which is about ten times that of the required value. Since the rigidity is modeled herein, the above mentioned variation could be compensated with the variation in I of the material. Having chosen the model material, the typical prototype dimensions of vegetal stems are fixed in the range of 100–400 mm. Accordingly, using the Froude model law of scaling, the rigidity with the scale factor of $[SF]^5$ – the base diameter for model vegetation – will fall in the range of 1.65–5.5 mm. The base diameter as established above only ensures that the bending action of the vegetal stems is properly scaled. Thus, the advantage of modeling rigidity rather than Young's modulus is clearly brought out. However, for accurate hydrodynamic interaction of the flow and stems, the hydrodynamic forces need to be correctly scaled according to Froude's Law. Considering the drag/inertia force regime (Chakrabarti, 1983), the corresponding diameters for the exposed part of vegetal stems were set. The variations in the stem diameters for the two different model cylinders are pictorially represented in Fig.1.

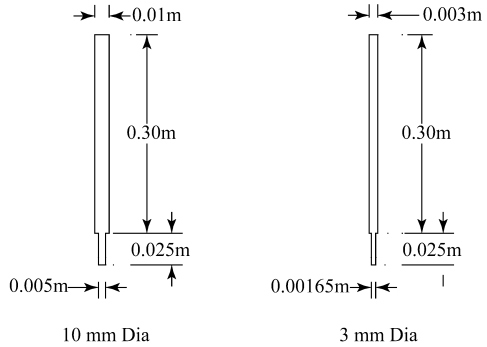

Fig.1 Typical configurations of vegetal stem

In order to ensure that the change in diameter does not affect the bending behavior of the model vegetation, a small clearance is provided between the base and the section, where the diameter changes from a lower to higher value as shown in the above figure. It is to be noted that the diameter at the root is used only for calculation of the EI of the vegetal stems.

4 Experimental details

4.1 General

The present experimental study was carried out in a wave flume 72 m long, 2.0 m wide, and 2.7 m deep at the Department of Ocean Engineering, Indian Institute of Technology, Madras, India. The flume of width (2 m) was partitioned longitudinally into three parts, each of which had a width of 0.66 m, so as to test all three configurations simultaneously.

A beam type single component force transducer (HBM) was used to measure the inline wave force on the model structure in the wave flume. The load cell with a measuring range of 200 N with an accuracy of 0.1 N housed inside the model structure with a dimension of 0.2 m×0.2 m and 0.3 m high is shown in Fig.2.

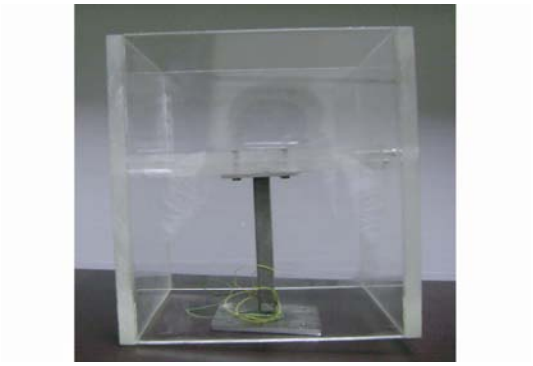

Fig.2 A view of the model with force transducer

4.2 Wave and vegetation parameters

The experiments were conducted for three different set-ups simultaneously. Each of the three compartments had a rigid bed with a slope of 1:30 starting from a distance of 28.5 m from the wave maker. The depth of water at the toe of the slope was maintained as 1.0 m. Three different widths of green belts at 0.250, 0.625, and 1 000 m, consisting of the vegetal stems fixed in a staggered arrangement were employed for the tests. For each of the staggered arrangements, two different diameters of vegetation at 10mm and 3 mm for each of the green belts as mentioned earlier were adopted.

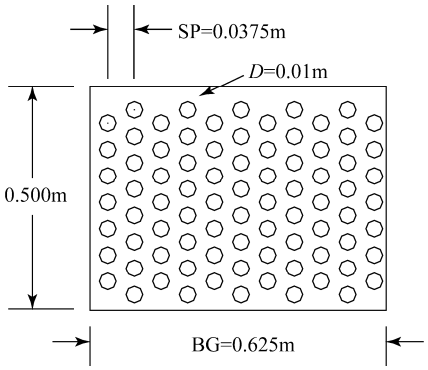

Fig.3 Schematic diagram of staggered configuration of green belt (SP = 0.037 5 m; BG = 0.625 m and D = 0.01 m)

Furthermore, for each of the two diameters considered, two different spacings of 37.5 mm and 75 mm were selected. Thus, for the present study, 12 different experimental setups were considered. A typical setup of vegetal stems for D = 10mm, SP = 37.5 mm, and BG= 0.625 m is shown in Fig.3. For the above mentioned 12 combinations of the vegetal parameters, tests to measure the forces on the model structure positioned at locations G/B = 0, 0.5, 1.0, and 1.5 were carried out.

The said tests were conducted in the absence and presence of the model green belt. The schematic representation defining the location of the structure and the green belt adopted for the study is shown in Fig.4. A block diagram showing the vegetal parameters, D, SP, and BG adopted for the tests along with the values of Vegetal Parameter BG×SP/D^2 achieved are projected in Fig.5.

4.3 Force measurements

A typical set-up for the measurement of forces on a structure in the absence of vegetation and with configuration of vegetation is shown in Fig.6(a). A closer representation of the test set- up is projected in Fig.6(b). A view of the said test set-up is shown in Fig.7.

The signals from the wave gauges and load cells through a wave amplifier were acquired simultaneously by a 12-bit resolution A/D card for a duration of 80 seconds and stored in a personal computer which was also used for driving the wave maker. The sampling interval for data collection adopted was 0.025 s. The measured wave and force time histories were subjected to time domain analysis for the peak values of forces F_{max}.

5 Results and discussion

5.1Validation of measurement of forces

The solution for forces on simple structures such as circular as well as non-circular cylinders is well documented in research literature. To commence the studies, initial tests with the model structure mentioned earlier instrumented with a load cell for measuring the in-line forces and rigidly fixed on the sloping bed without the vegetation were subjected to waves of different frequencies and heights. The measured forces compared with the solution of Isaacson (1979) in Fig.8 exhibit a reasonable agreement, thus validating the measurement of forces.

The forces exerted on the model structure due to cnoidal waves with a moderate to high Ursell parameter, $Ur = HL^2/h^3$, e.g., from 18 to 700, have been measured in the absence and presence of vegetation on the seaside. In order to make the presentation of results meaningful while permitting a direct application of model results to the field, the force is expressed in a dimensionless form as $F^*= [F_{max}/(0.5\rho g H^2 B_s)]$. The variation of dimensionless force with reduced velocity V_r is investigated.

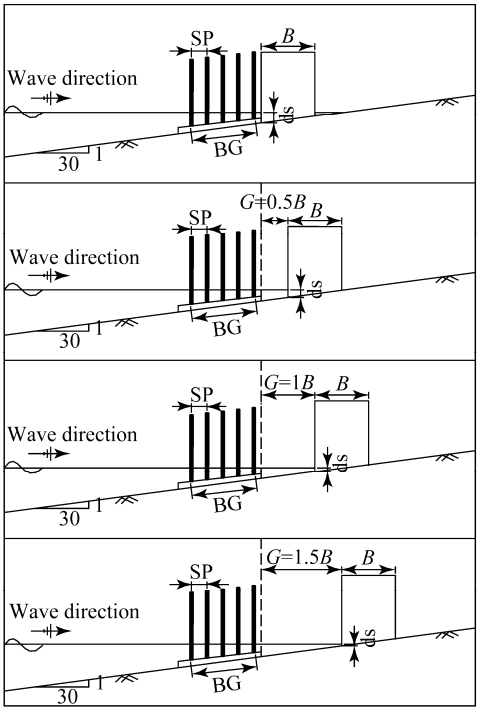

Fig.4 Definition of variables for force measurements in the wave flume (Presence of vegetation)

The KC number is usually defined as $(U_{max}T)/D$, wherein, U_{max} is approximated as $c= [gh_s(1+(H/h_s))]^{0.5}$ (Wiegel, 1964) and $D = B_s$ which is the breadth of the structure normal to the wave direction. As stated earlier, the tests were carried out with Cnoidal waves of four different periods, the results of which are discussed below.

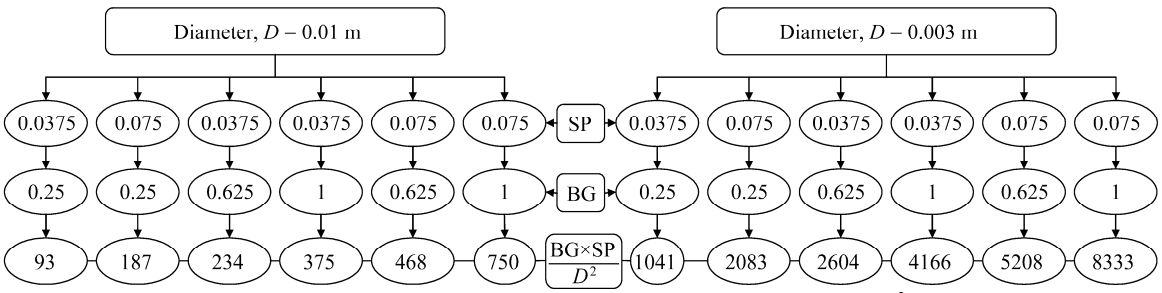

Fig.5 Block diagram showing the vegetal parameter, BG×SP/D^2

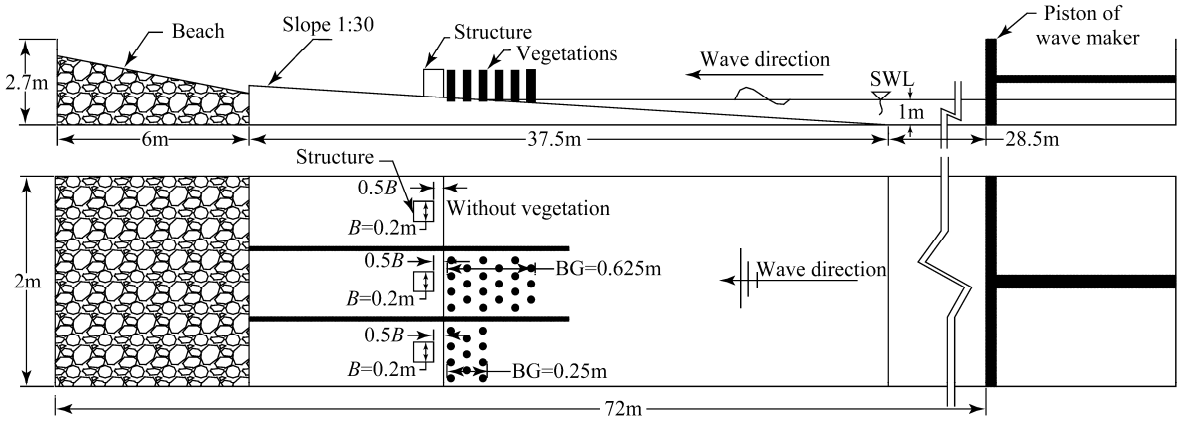

(a) Plan and sectional views of the flume with the test set-up

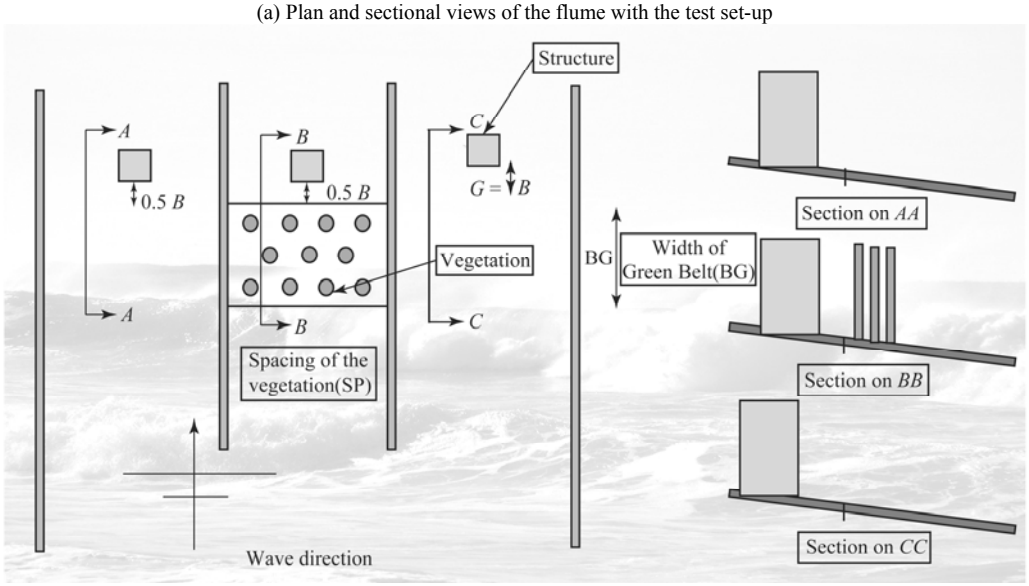

(b) A closer view of the test section

Fig.6 Experimental set-up for force measurements in the wave flume for *G*/*B*=0.5 and 1

5.2Variation of dimensionless force with *KC*

5.2.1 Reduced velocity, V_r of 11 to 14

The variation of dimensionless force, *F** with a *KC* number for a finite range of BG/SP between 3 and 8 for four values of *G*/*B* are shown in Fig.9. These plots have been prepared for constant values of h_s/gT^2. The results thus obtained for the forces on the structure, in the presence and absence of the green belt, are superposed in each of the plots. In order to understand the effect of vegetation on the forces, open symbols are used for the case of results without vegetation and filled symbols are used for the results with vegetation. The tests have covered a wide range of *KC* numbers (up to 140).

The results clearly show that in general, the force *F** decreases with an increase in the KC number for each of the h_s/gT^2 tested. For *G*/*B*=0 (structure adjacent to the green belt), reduction in the forces by 50 to 95 percent is observed for the range of *KC* numbers considered. For *G*/*B*=0.5 (structure is at 0.5*B* from the green belt), although the trend in the variation of *F** with a *KC* is similar to that for *G*/*B*=0, it is observed that the forces on the structure increased up to a maximum of 75% with the presence of vegetation compared to instances without the vegetation. The probable reason for the increase in forces with the presence of vegetation could be that the waves, after propagating through the vegetation, undergo re-reflection in the space between the model building and the vegetation leading to the increase in energy density in the vicinity of the structure, thereby increasing the forces on the structure. With an increase in *G*/*B* to 1.0, the difference between the forces on the structure in the presence and absence of vegetation tends to lessen (when compared to the case of *G*/*B*=0.5). The said trend is observed to continue for a further increase in *G*/*B* to 1.5, thus suggesting that as the distance between the green belt and the structure increases, the energy density in the gap is reduced leading to a reduction in the forces. From the above study it is inferred that the forces on the structure will be further reduced to a greater extent with a further increase in *G*/*B* beyond 1.5. Hence, it may be suggested that the ideal location of the green belt is either immediately before the structure or greater than twice the width of the structure.

The variation of dimensionless force F^* with a KC number for the next range of BG/SP from 13 to 17 and for 26 are shown in Figs.10 and 11, respectively. It is observed the trend in the variation of F^* with a KC number for all h_s/gT^2 and for all G/B is found to be as discussed above. In most of the above-mentioned plots, it is seen in general that for a larger BG/SP, F^* is found to be less because of attenuation being offered over a larger distance for a higher BG.

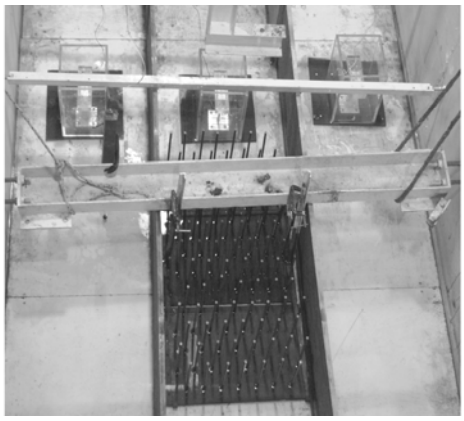

Fig.7 A view of the test set-up for different G/B

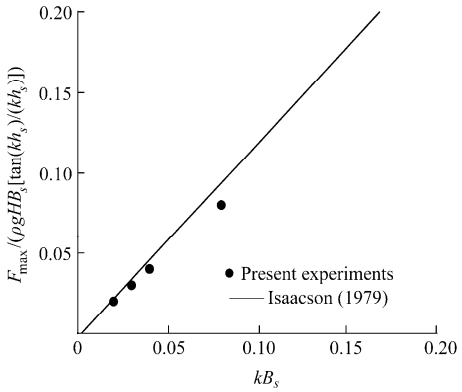

Fig.8 Comparison of present experimental results with Isaacson (1979)

5.2.2 Reduced velocity, V_r of 130 to 166

The variations of dimensionless force F^* with a KC number are plotted in the same way as shown above for finite ranges of BG/SP and G/B. These results of BG/SP for the ranges 3 to 8, 13 to 17, and 26 are brought out in Figs.12, 13, and 14, respectively. It is observed that the variation in F^* is quiet similar to that observed for $11 \leq V_r \leq 14$. In general the forces with vegetation appear to be marginally (about 20%–40%) lower than those for $11 \leq V_r \leq 14$. The bending effect for higher V_r is expected to be greater resulting in higher drag due to which attenuation will be greater.

h_s/gT^2	0.0004	0.0001	0.00004	0.00002
No Veg.	◇	○	□	△
Veg.	◆	●	■	▲

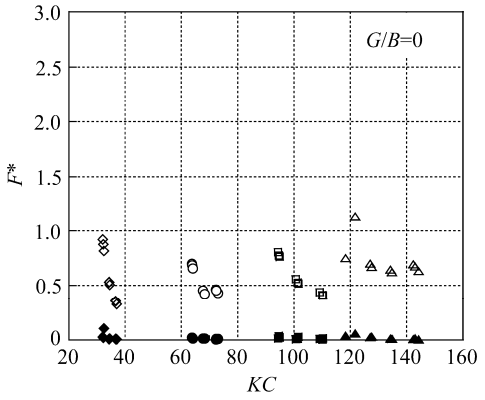

(a) G/B=0

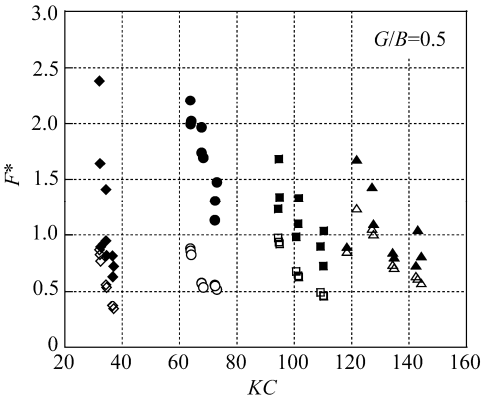

(b) G/B=0.5

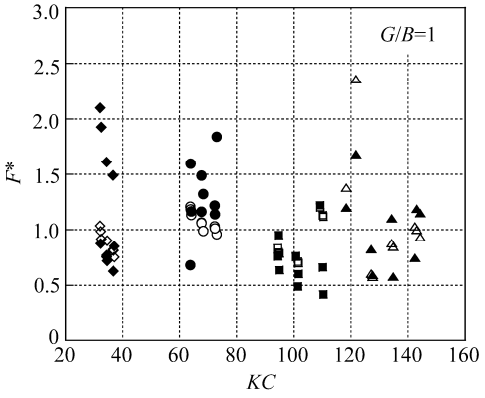

(c) G/B=1

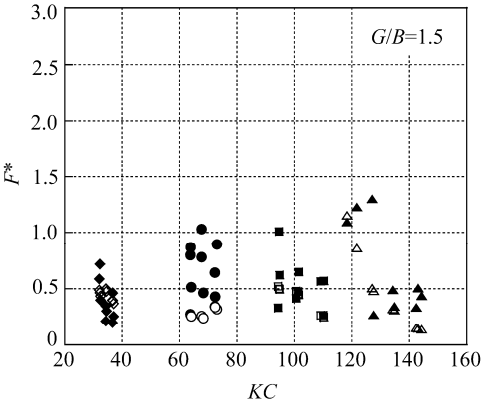

(d) G/B=1.5

Fig.9 Variation of dimensionless force with KC number for [V_r = 11 to 14] and BG/SP = 3 to 8

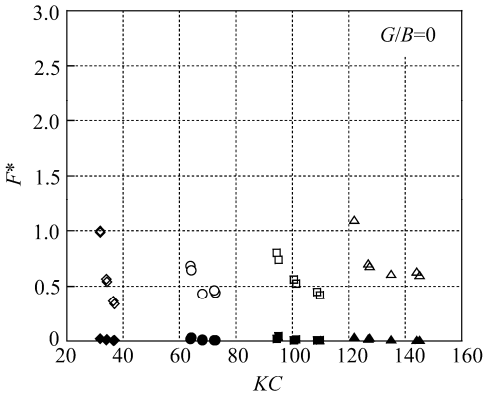

(a) G/B=0

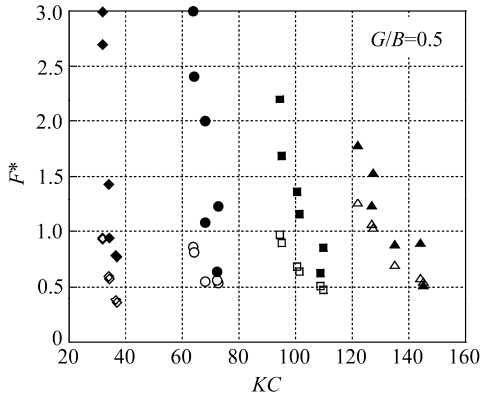

(b) G/B=0.5

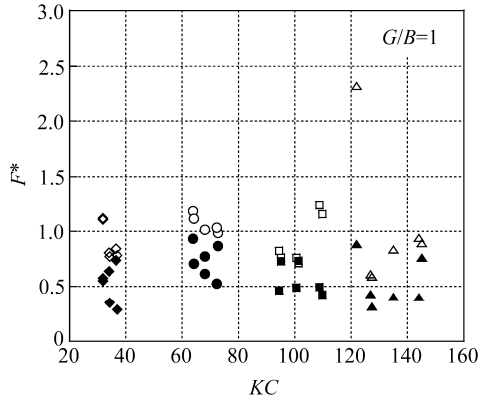

(c) G/B=1

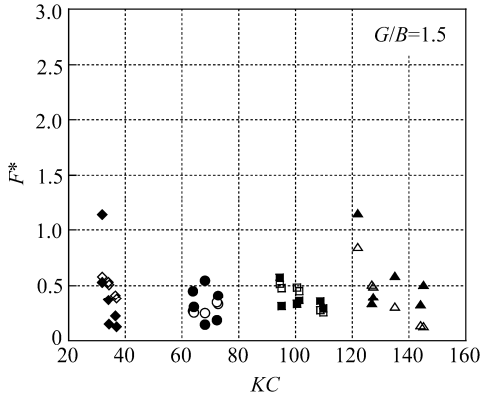

(d) G/B=1.5

Fig.10 Variation of dimensionless force with *KC* number for [V_r = 11 to 14] and BG/SP = 13 to 17

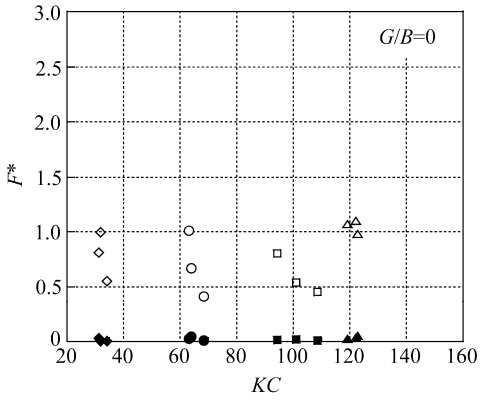

(a) G/B=0

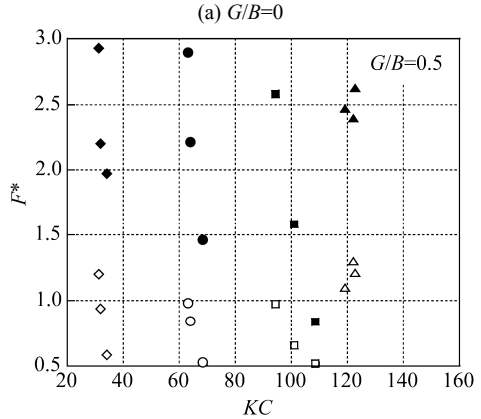

(b) G/B=0.5

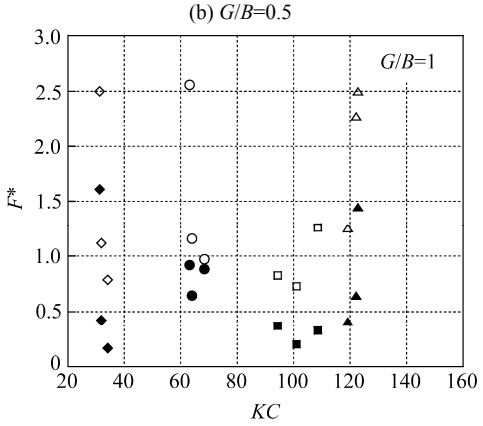

(c) G/B=1

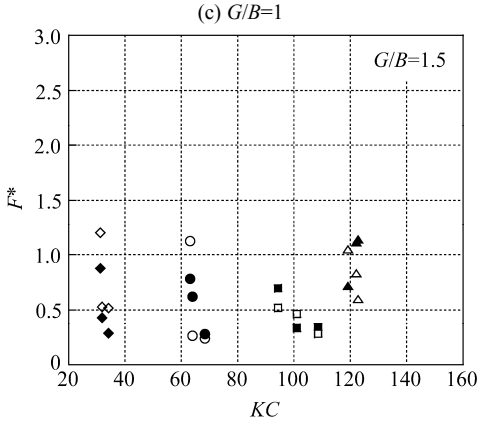

(d) G/B=1.5

Fig.11 Variation of dimensionless force with *KC* number for [V_r = 11 to 14] and BG/SP = 26

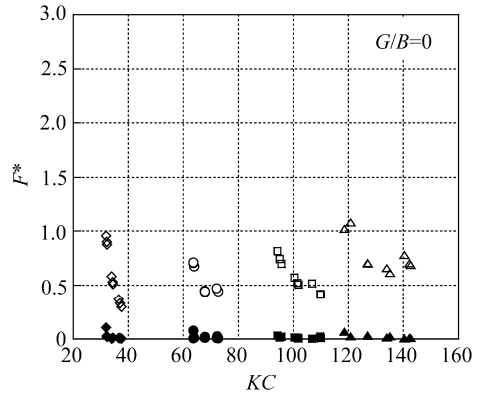

(a) *G*/*B*=0

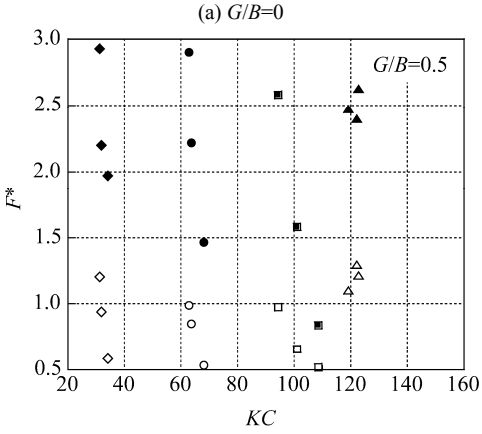

(b) *G*/*B*=0.5

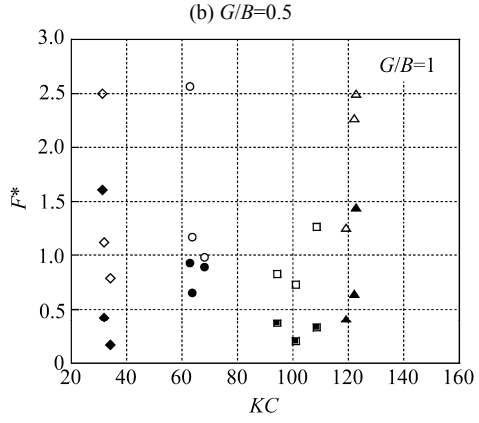

(c) *G*/*B*=1

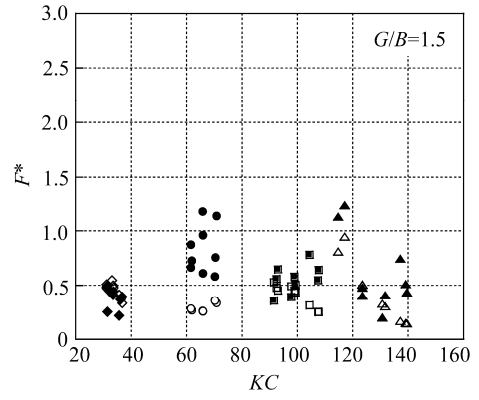

(d) *G*/*B*=1.5

Fig.12 Variation of dimensionless force with *KC* number for [V_r = 130 to 166] and BG/SP = 3 to 8

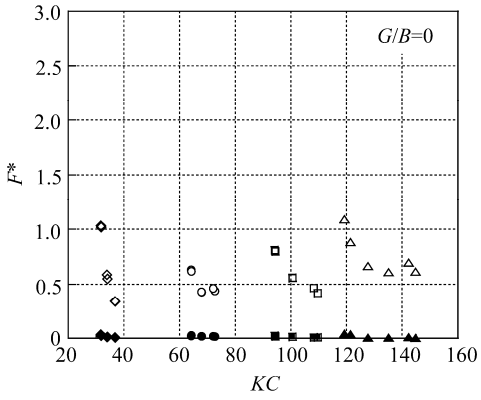

(a) *G*/*B*=0

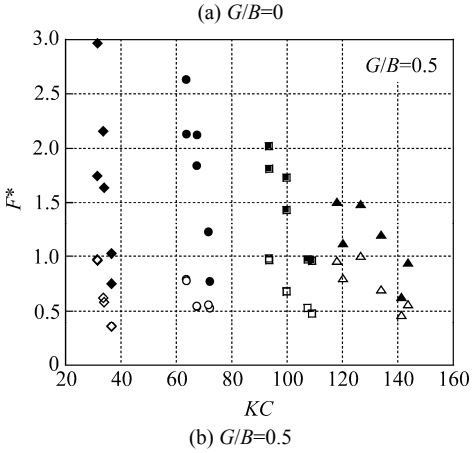

(b) *G*/*B*=0.5

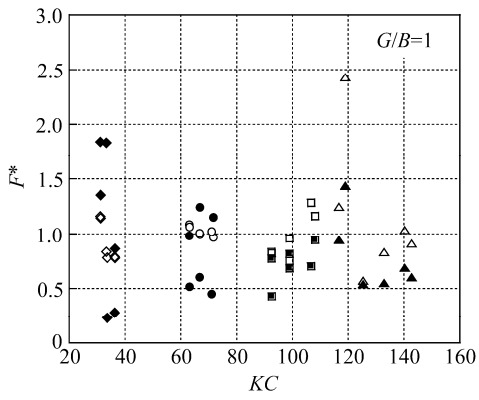

(c) *G*/*B*=1

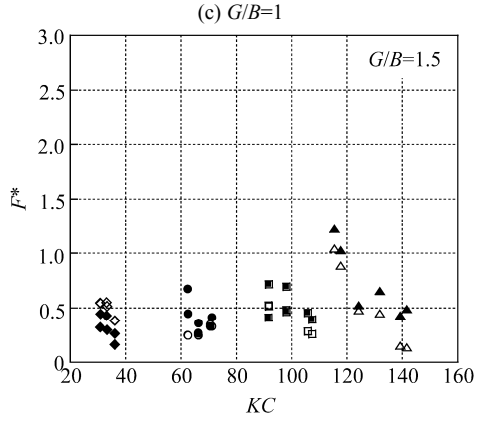

(d) *G*/*B*=1.5

Fig.13 Variation of dimensionless force with *KC* number for [V_r = 130 to 166] and BG/SP = 13 to 17

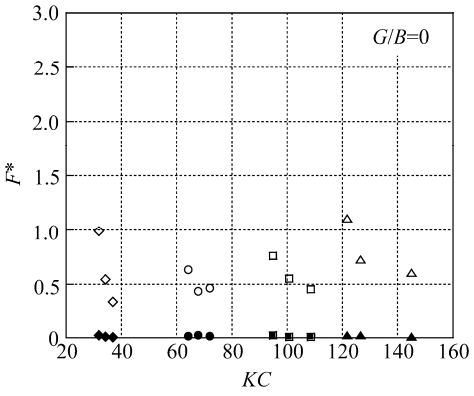

(a) G/B=0

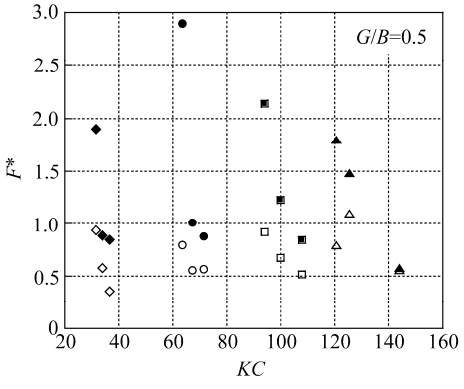

(b) G/B=0.5

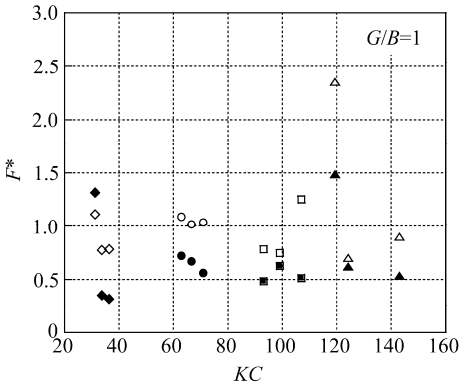

(c) G/B=1

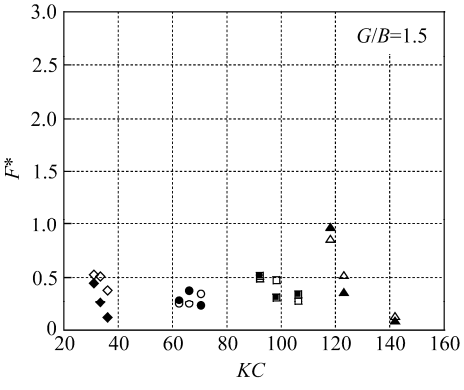

(d) G/B=1.5

Fig.14 Variation of dimensionless force with *KC* number for [V_r = 130 to 166] and BG/SP=26

5.3 Percentile analysis on F^*

The experimental data on F^* was subjected to a percentile analysis in order to clearly see the effect of G/B. The variations of the percentage of occurrence of F^* in the absence and presence of the vegetation are plotted in Figs.15(a) and (b), respectively. The percentage of occurrence is used here as a means of knowing the "percentage of test cases", among all conditions studied, for which the force on the model building is lower than a certain value. This is demonstrated by the following example.

For the case with the absence of vegetation in Fig.15(a), the percentage of occurrence of $F^* \leq 1.0$ is found to be about 92%, 90%, 55%, and 96%, respectively for G/B =0.0, 0.5, 1.0, and 1.5. This indicates that for a condition of no vegetation the force is at its maximum for G/B=1.0 and beyond which it is reduced.

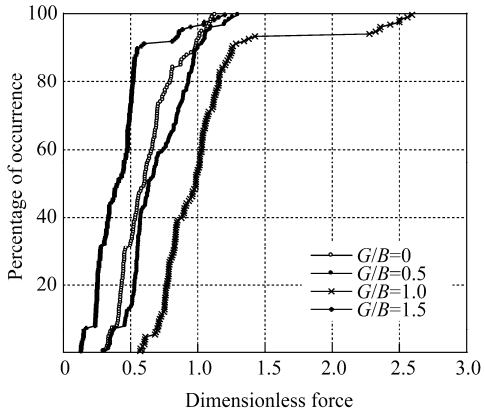

(a) Percentage of occurrence of force in the absence of vegetation

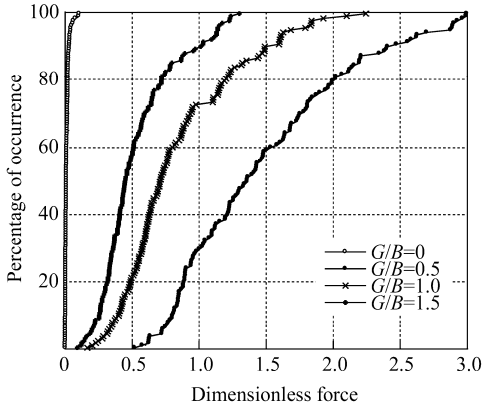

(b) Percentage of occurrence of force in the presence of vegetation

Fig.15 Probability distribution of dimensionless wave forces in experimental data for the absence and presence of vegetation

Extending this analogy to the cases of a model building fronted by vegetation for a reference force of $F^* \leq 1.0$, the percentile for G/B=0.0, 0.5, 1.0, and 1.5 is 100%, 30%, 75%, and 90%, respectively. Considering the fact that all experiments are conducted for high Ursells numbers ($U_r \geq 180$), the above discussion indicates that G/B=0 and G/B>1.5 will certainly be beneficial.

Out of the four *G/B*=0, 0.5, 1, and 1.5 tested, forces seemed to be very low only for the cases of *G/B*=0 and *G/B*=1.5. This is mainly due to the frictional resistance offered by the slope as the jet of water runs off by a distance from the reference line and the energy already lost in the green belt. However, for the case of *G/B*=0.5 and *G/B*=1, the jet of water running up the slope may have significant re-reflection and energy density might be equivalent to 2*H* (where *H* is the wave height). As the run-up height increases, unlike the other two cases of *G/B* of 0 and 1.5, the forces are higher, particularly for *G/B*=0.5 and 1.

When vegetation is placed in front of the structure, the waves passing through the vegetation over a slope are expected to amplify due to the resistance offered by the vegetation. This is associated with splashing as observed during the experimental program. In the case of *G/B*=0.5 and 1.0, the mass of water which impinges on the structure exerts larger forces. The afore-mentioned impingement and splashing was observed to be significant for the tests with *G/B*=0.5 and *G/B*=1.0, leading to larger forces. For the tests with *G/B*=0, there is a gradual pileup of water, and impingement does not occur. This results in the lowest of forces.

6 Summary and conclusion

The results of the variation of forces on a structure positioned at different distances from the green belt and subjected to the action of Cnoidal waves as a function of non-dimensional flow and vegetation parameters were presented and discussed in detail in this paper. The effects of a *KC* number, VFP, V_r, BG/SP, and *G/B* have been investigated. The BG/SP parameter has been found to be very useful in understanding the effects of placement of vegetation in combination with the width of the green belt on the forces F^*. On the other hand, *G/B* = 0 or *G/B*>1.5 has been found to be suitable for the green belt to be effective, while *G/B*=0.5 has been found to have an adverse effect. Considering the value of $F^* \leq 1.0$, the vegetal patches have been able to limit the forces by a percentile of 92%, 90%, 55%, and 96%, respectively for *G/B* =0.0, 0.5, 1.0, and 1.5. Also, Behind vegetal patches, the force is at its maximum for *G/B*=1.0 and beyond which the forces start to diminish.

References

Augustin LN, Irish JL, Lynett P (2009). Laboratory and numerical model studies of wave damping by emergent and near emergent wetland vegetation. *Coastal Engineering*, **56**(1), 332-340.

Chakrabarti SK (1983). *Hydrodynamics of offshore structures*. Computational Mechanics Publications, Southampton, Boston, 326.

Danielsen F, Soresen MK, Olwig MF, Selvam V, Parish F, Burgess ND, Hiraishs T, Karunagaran VM, Rasmussen MS, Hansen LB, Quarto A, Sriyadiputra N (2005). The Asian tsunami: a protective role for coastal vegetation. *Science*, **310**(5748), 643.

Harada K, Imamura F (2005). *Effects of coastal forest on tsunami hazard mitigation–a preliminary investigation*. Tsunamis, Case Studies and Recent Developments, Springer, Netherlands, 279-292.

Hiraishi T, Harada K (2003). Greenbelt tsunami prevention in South Pacific region. *Report of the Port and Airport Research Institute*, Yokosuka City, Kanagawa.

Hiraishi T (2005). Greenbelt technique for tsunami disaster reduction. *APEC-EqTAP Seminar on Earthquake and Tsunami Disaster Reduction*, Jakarta, Indonesia, 1-6.

Irtern E, Gredik N, Kabdasli MS, Yasa NE (2009). Coastal forest effects on tsunami run-up heights. *Ocean Engineering*, **36**, 313-320.

Issacson M (1979). Wave force on large square cylinders. In *Mechanics of Wave-induced Force on Cylinders*, Ed. T. L. Shaw, London, 609-622.

Kathiresan K, Rajendran N (2005). Coastal mangrove forests mitigated tsunami. *Estuarine Coastal and Shelf Science*, **65**(3), 601-606.

Kongko W (2005). Mangrove as a tsunami reduction and its application. *APEC-EqTAP Seminar on Earthquake and Tsunami Disaster Reduction*, Jakarta, Indonesia.

Nandasena KNA, Tanaka N (2007). Elucidating effectiveness of dominant types of coastal vegetation found in Sri Lanka for tsunami protection in numerical modeling. *Annual Research Journal of SLSAJ*, **6**, 16-21.

Struve J, Falconer RA, Wu Y (2003). Influence of model mangrove trees on the hydrodynamics in a flume. *Estuarine, Coastal and Shelf Science*, **58**(1), 163-171.

Sundar V, Sannasiraj SA, Murali K, Sundaravadivelu R (2007). Run-up an inundation along the Indian Penninsula including Andaman Islands due to great Indian ocean tsunami. *Journal of Waterway, Port, Coastal, and Ocean Engineering*, **133**(6), 401-413.

Tanaka N, Sasaki Y, Mowjood MIM, Jinadasa KBSN, Homchuen S (2007). Coastal vegetation structures and their functions in tsunami protection: experience of the recent Indian Ocean tsunami. *Landscape and Ecological Engineering*, **3**(1), 33-45.

Tanino Y, Nepf HM (2008). Laboratory investigation of mean drag in random array of rigid, emergent cylinders. *Journal of Hydraulic Engineering*, **134**, 34-41.

Wiegel RL (1964). *Oceanographical engineering*. Prentice-Hall, Inc, Englewood Cliffs, USA, 65.

Dr. Noarayanan Lakshmanan is presently a research fellow at the Nanyang Technological University, having obtained his PhD from Indian Institute of Technology. He has intensively researched on flow-vegetation interaction and speciailses in experimental techniques.

Dr. Murali Kantharaj is presently a professor at the Department of Ocean Engineering, Indian Institute of Technology Madras (www.oec.iitm.ac.in). Dr. Murali specialises in computational hydrodynamics, modelling of nearshore processes and high performance computing. With more than 100 peer reviewed papers in the areas of Coastal and Ocean Engineering, he has advised more than 25 postgraduate students including 9 PhDs. He may be contacted at murali@iitm.ac.in.

Dr. Vallam Sundar is presently a professor at the Department of Ocean Engineering, Indian Institute of Technology Madras (www.oec.iitm.ac.in). He has published about 100 papers in International journals and has about 300 papers in Conferences and national journals. He served as the Chairman of IAHR–APD from 2006 to 2010. His field is coastal engineering, harbor related problems and tsunami mitigation measures and has supervised 17 PhDs.